PFC/RR-87-13 DOE/PC-70512-8

Development and Test of an Internally Cooled, Cabled Superconductor (ICCS) for Large Scale MHD Magnets

Semiannual Progress Report

Period from January 1, 1986 to June 30, 1986

Becker, H., Dawson, A.M.,
Hatch, A.M., Marston, P.G., Tarrh, J.M.,

Plasma Fusion Center
Massachusetts Institute of Technology
Cambridge, Massachusetts 02139, USA

This work was supported by the U.S. Department of Energy, Pittsburgh Energy Technology Center, Pittsburgh, PA, 15236 under Contract No. DE-AC22-84PC70512.

TABLE OF CONTENTS

1.0 Introduction

A three-year program to develop and test an internally-cooled cabled superconductor (ICCS) for large-scale MHD magnets is being conducted by MIT for the Pittsburgh Energy Technology Center (PETC) under Contract DE-AC22-84PC70512. The program consists of the following four tasks:

I. Design Requirements Definition

II. Analysis

III. Experiment

IV. Full-Scale Test

This report summarizes the technical progress during the period from January 1,1986 to June 30, 1986.

The objective of Task I is to establish the design requirements definition for full-scale conductors for use in early commercial MHD magnets. Since the focus of MHD power train development is fixed now on relatively small systems such as may be used in retrofit applications, the work concerns conductors suitable for systems of that size and type.

The objective of Task II is to accomplish the analysis required to substantiate the design for the full-scale conductor, and to provide the background for defining an experimental test program (Tasks III and IV).

The objective of Task III is to perform experiments with subscale conductors to verify the efficiency of the design concepts considered and also the accuracy of predictive analysis.

The program is directed specifically toward the development of ICCS because this type of conductor has many significant advantages over bath-cooled conductors for the MHD application: relatively higher stability margin, greater electrical integrity (because the conductor can be wrapped with continuous insulation), greater mechanical integrity and durability, and the elimination of a heavy-walled liquid helium containment vessel. The concept offers great promise in resolving the issues of constructability and long-term durability for commercial MHD magnets while minimizing the overall costs and risks of such systems.

In order to establish a conductor Design Requirements Definition, it is necessary to know the design characteristics of the magnet in which the conductor is intended to operate. Since a suitable reference design for a retrofit-size MHD magnet did not exist when the program was started, the development of a preconceptual design for such a magnet has been a major part of the Task I effort.

2.0 Review of Technical Progress Prior to June 30,1986

A brief review of technical progress from the start of the program through June 30, 1986 is provided below as a background for the report of progress contained in Sections 3.0 and 4.0.

As a starting point for preconceptual magnet design, it was assumed that the typical retrofit-size MHD magnet will:

a. accommodate a supersonic MHD channel of about 35 MWe output, requiring a peak on-axis field of 4.5 T.

b. operate at a design current in the neighborhood of 25 kA.

As a baseline for conductor design, it was assumed that the dimensions and construction of the conductor would be the same as of those of the ICCS conductor used in the large D-shape magnet designed and built by Westinghouse for the fusion Large Coil Program (LCP), described in Reference 2. This was done to take advantage of the manufacturing technology that had been developed for that project. The MHD conductor will, however, use niobium titanium (NbTi) superconductor rather than niobium tin (Nb_3Sn).

The selection of magnet size and field strength is supported by information obtained from the MHD community as reported previously[1]. The selection of a relatively high design current is in the interest of minimum overall system cost, based on information provided in Reference 3. The selection of the particular ICCS overall dimensions and construction is aimed at minimizing conductor development time and cost by using a conductor size and construction for which production and tooling experience already exist.

An initial preconceptual design for a retrofit-size magnet was generated, incorporating a 60° rectangular saddle-coil winding of ICCS, without substructure, operating at a design current of 24 kA and surrounded by a stainless-steel force containment structure and cryostat.

A detailed computer analysis of the winding showed maximum fields to be substantially higher than originally estimated (approaching 7.2 T instead of the estimated 6 T), requiring that the design be modified to reduce the maximum field and assure stable operation.

Several winding design modifications, aimed at reducing the maximum field, were then analyzed. Modifications included changing the shape of the end turns, changing the aspect ratio of the winding cross section, and decreasing the winding average current density. A reduction of maximum field to below 6.9 T was found to be possible. A revised winding design having an increased thickness, an increased bend radius in the end turns, and a lower current density was established as most suitable for the application. Characteristics of the revised design and also of the original design are given below:

	Original	Revised
Coil Thickness (m)	0.24	0.305
Minimum End Turn Bend Radius (m)	0.15	0.30
Winding Average Current Density (A/cm^2)	3900	3200
Design Current in Conductor (kA)	24	18
Maximum Field in Winding (T)	7.2 (Orig. est. 6.0)	6.9

The end product of the work was an improved magnet preconceptual design which compared favorably with earlier magnet designs in reliability, manufacturability, and cost-effectiveness, together with a draft Design Requirements Definition for the conductor that represents a sound basis for continued development and proof-testing of subscale conductor elements as well as a full-scale conductor prototype.

Subsequent iterative analyses of the magnet, conductor and refrigeration system have identified critical design and conductor test issues which have begun to be addressed during the period reported herein.

3.0 Summary of Technical Progress, January 1 to June 30, 1986

During this period the negotiations where completed to extend the period of performance of this work to December 31, 1987. The cause of the extension is reduced funding rate. The extension was agreed to without additional cost; it should, however, be noted that additional such delay will incur stretch-out cost.

As has been noted in the previous reports the purpose of the conceptual magnet design effort is to establish the operating conditions and requirements for the conductor. The effort during this period focused particularly on the detailed structural behavior of the ICCS conductor under the predicted design load. The detailed stresses, deformations etc., of the conduit (conductor sheath) under the influence of transverse, electromagnetic loading have been calculated and found to be satisfactory if the coil is "potted."

A test plan has been developed and analysis of the selected test conductors has begun.

Analysis to date has also clearly identified the truly unique advantage of the ICCS configuration for DC applications. The process and considerations for thermodynamic stabilization of this conductor are fundamentally different from any of the prior art, and as a result may enable a conductor design having important additional advantages beyond those already identified.

4.0 Results of Design and Analysis Effort

4.1 Structural Behavior of ICCS

4.1.1 Load

The ICCS (both cable and sheath) will be subjected to the following loads: (1) longitudinal loads arising from electromagnetic forces on the coil "saddle;" (2) transverse electromagnetic loads; (3) internal pressure loads including the high transient pressures which can occur during a quench, and thermal stresses which can occur during cooldown and warm-up of the coil structure.

There is little problem predicting response to the longitudinal loads, therefore the principle focus of this analysis has been confined to transverse loading.

The transverse Lorentz force on each conductor is transmitted to its neighbor and thus accumulates to a peak value which is in the vicinity of the zero field point in the overall winding cross section. For the reference design case this value has been determined to be 7,250 pounds per inch which is assumed to act on the top surface of a conductor under working conditions.

There are a variety of factors which influence the stiffness, stress distribution and strength of an ICCS. These include: (1) cable composition, cable winding details and the degree of compaction; (2) conduit cross-section shape and dimensions; (3) conduit material.

There are also a variety of winding design parameters which can have a large influence on the operating stress distribution in the conduit. In particular, these would include the thickness and stiffness of potting material used to fill the corners between adjacent turns and winding layers. The stiffness of lateral restraint orthogonal to the loading direction is also very important. The coefficient of friction between adjacent turns and restraining walls may also have an influence.

Of particular interest is the behavior in the corner of the conduit. Representation of the load, movement and deformation of the corner are shown in Figures 1 and 2.

The following finite element analysis depicts the general behavior of an ICCS conduit without an internal cable. The features of primary interest are the locations and magnitudes of the peak stresses and the effective transverse stiffness of the conduit.

The results are presented in reproductions of the computer printouts. The deflection and stress scales are included.

Shape and Material Properties of Conductor and Potting Epoxy

The geometrical shape of one-quarter of the conductor is shown in Figure 3. The conductor is assumed to be made of stainless steel with the physical properties of

Young's modulus (E) = 30 msi

Poisson's ratio (ν) = 0.3

Yield stress (σ_y) = 140,000 psi

It was also assumed that the stress-strain curve of the material can be represented by

$$\epsilon = (\sigma/E)\,[1 + (3/7)(\sigma/\sigma_y)^7].$$

The potting is done as shown in Figure 4 by epoxy with the physical properties of Young's modulus = 0.6 msi and Poisson's ratio = 0.3, unless otherwise indicated.

Element Discretization

A quarter of the conductor is approximated by plane stress quadratic elements. Except when otherwise specified in the individual cases, the element and node numbers are shown in Figures 5 and 6 for a loose conductor and in Figures 7 and 8 for a potted conductor, respectively. Only a quarter of the conductor is analyzed because it has two planes of symmetry in both load and shape configuration.

Loading Pattern

A uniformly distributed pressure of 7250 lb/in is assumed to act on the top surface of the conductor under working conditions. However, in the case of a loose conductor, this load may be reduced to a concentrated load acting at Node 4 as shown in Figure 6, or it may be distributed over a reduced area in the case of a potted conductor, as shown in Figure 8 and enlarged in Figure 9.

When the term "working load" is used in this report, it refers to the loading pattern described in this section.

Displacement Boundary Conditions

The conductor is prohibited to move in the x-direction at Section A-A or in the y-direction at Section B-B, as shown in Figures 6 and 8. The side surfaces are assumed to be partially fixed if rigid side supports are imposed, or a mixed boundary condition of displacement and force may occur in the case of flexible side supports.

Elastic - Plastic Analysis of the Loose Conductor

Since rigid side supports will be assumed in this analysis, applied loads reduce to a concentrated load at the transition point between the flat and curved sections of the conductor, as shown in Figure 6. Six load cases were considered. Their magnitudes in pounds are 500, 1000, 1500, 2000, 2500, and 3000, respectively. Table 1 gives a summary of the results of both elastic and plastic analyses.

Table 1. **The Variation of Equivalent Stress and Deformation with Respect to the Applied Load as the Load Increases from Elastic to Plastic Range in the Case of a Flat Conductor with a Concentrated Top Load at Node 4 and Rigid Side Supports at Node 8 and 623, Loose Packing, That Is, No Epoxy, Conductor Only**

(1)	(2)	(3)	(4)	(5)	(6)
	1E+5	1E-3	1E-3	1E+5	1E+5
500	8.5351	0.5858	0.5858	0.405	0.405
1000	8.5077	1.1715	1.1715	0.810	0.810
1500	7.8575	1.7573	1.7669	1.215	1.21
2000	6.1752	2.3430	2.4831	1.62	1.50
2500	4.7138	2.9288	3.4122	2.025	1.65
3000	4.1505	3.5146	4.5690	2.43	1.81

Titles of the columns:

(1) The magnitude in pounds of the concentrated load at node 4 in the opposite y direction.

(2) The equivalent tangent modulus in psi in the y-direction of the conduit calculated by using the loads in column (1) and the deformations in column (4).

(3) The displacement in inches of node 4 in the opposite y-direction calculated by assuming only elastic deformation happens.

(4) The displacement in inches of node 4 in the opposite y-direction calculated by taking both elastic and plastic deformations into consideration.

(5) The elastic stress in psi at the most stressed element.

(6) The equivalent stress in psi at the most stressed element.

The force-deformation curve (which can also be converted to the stress-strain curve by dividing both the x and y axes by a scale of 0.409) is shown in Figure 10. This curve is obtained by passing a natural spline through the six calculated data points. Local yielding does not happen until the magnitude of load is over 1000 pounds. Thereafter, the effect of the plastic strains is appreciable.

The equivalent tangent modulus-force curve is obtained by approximating the force-deformation curve with 120 straight line segments and using the slopes of these segments as tangent moduli. The tangent modulus-force curve is plotted in Figure 11. It can be seen that the tangent modulus decreases rapidly after the magnitude of the load increases above 1000 lbs.

The stress variation across the critical section (Section C-C in Figure 6) under the working load (approximately equivalent to a concentrated load of 2965 lbs) is shown in Figure 12. The deformed shape of the conductor is shown in Figure 13.

Analysis of the potted conductor indicates a reduction in maximum equivalent stresses to approximately 65% of a loose conductor. The winding composite should thus be struc-

turally adequate to support the design loads. This will be confirmed by suitable verification tests.

As will be discussed in the next section both the structural and thermal analysis of ICCS predict the possibility of a new design having important advantages for MHD.

4.2 Test Conductor Analysis

The previously existing software for the analysis of ICCS windings has proved to be inadequate for the determination of their behavior under DC conditions. The new analysis being performed under this contract has established a unique advantage of ICCS for applications in which the dominant source of thermal perturbations is frictional heating.

The situation for MHD is quite different than that of a fusion reactor wherein windings must be able to accommodate large and rapid changes in field strength arising from ohmic heating pulses, plasma disruptions, and so forth. This rapid $\dot{B}$ creates AC heating directly in the multifilamentary composite strand. If such transient heating is adequate to raise the temperature of the conductor above the transition temperature of the superconductor, heat must be transferred through the conductor surface to the surrounding liquid helium at a rate such that the normal region of the superconductor will recover rather than propagate along the conductor length. A variety of factors conspire to limit both the transient heat transfer rate and the volume of helium coolant (enthalpy) available to absorb heat. At very low temperatures it is only the enthalpy of the helium coolant which plays a significant role in thermal stabilization of the superconductor, and for fast transients this is further limited to only the volume of helium which is in intimate contact with the conductor. In all cases, heat transfer rates are low and the required cooling surface area is correspondingly large. An MHD magnet, however, can be designed in such a way that the only significant source of heating in the conductor is the pulse of frictional heat which occurs when a conductor slips with respect to a neighboring surface. This heat is obviously generated at the outer surface of the insulated conductor and must penetrate through the electrical insulation and conduit (sheath) in order to heat the helium coolant, which in turn must be uniformly heated to above the superconductor transition temperature before a normal region can occur. In this case transient heat transfer limits are beneficial and the total enthalpy of all conductor components are not only available to stabilize against thermal perturbations but must, in fact, be "used" before a transition can occur.

Another difference relates to both magnet protection and to the size and weight of

the force containment structure. In all magnets where a significant amount of AC heating is possible, and also in pool-cooled DC magnets where frictional heat has a direct path to the copper/superconductor composite, it is important that the stabilizer (usually copper) has very good electrical conductivity (to reduce joule heating during current sharing). In the case of partially stable magnets, conductor design criteria relate to the enthalpy available below the transition temperature (the energy margin) and to the total thermal mass available to absorb energy stored in the magnetic field.

For a conductor as proposed in Figure 14, the energy margin is established primarily by the volume of helium in the conduit and can be very large compared to comparable pool-cooled configurations. Once this limit is reached and the magnet quenches, the normal conductor available to limit maximum temperature, (perhaps as high as 500 K), does not require very good conductivity. It is thus practical to consider a high-strength alloy of only moderate conductivity as the protection component of what is normally considered the stabilizing conductor and furthermore, to use this material as the conductor sheath.

A variety of high-strength alloys can be considered for the sheath, including dispersion-strengthened copper, microcomposites and aluminum alloys such as 2219-T81. A perforated thermal barrier between the cable and the sheath will further isolate the multifilamentary strands from the source of frictional heat without significantly impairing sheath-to-helium heat transfer. This "outside-in" thermal behavior of ICCS in DC devices is fundamentally different from all other superconducting winding composites and results in a situation wherein the heat transfer characteristics which normally limit "getting the heat out" and thus degrade stability now limit "getting the heat in" and have the opposite effect. It also permits simple design control of conductor energy margin and decoupling of protective conductor from stabilizing conductor. The latter, in turn, permits use of high-strength (moderate conductivity) protective conductor which can simultaneously provide a large fraction of the required structural support.

4.3 Test Plan Development

During this period work has progressed on the development of a Test Plan. A preliminary draft is attached. Additional effort is necessary to ensure adequacy of the test equipment and procedure to model "frictional heating" at the outer surface of the ICCS.

5.0 References

1. Quarterly Progress Report, Oct. 1, 1984 to December 31, 1984, Develop and Test an ICCS for Large Scale MHD Magnets, MIT, March 1985 DOE/PC-70512-2.
2. Technical Progress Report, period from January 1, 1985 to June 30, 1985, Develop and Test an ICCS for Large Scale MHD Magnets, MIT, November 1985, DOE/PC-70512-4.
3. Technical Progress Report, period from July 1, 1985 to December 31, 1985, Develop and Test an ICCS for Large Scale MHD Magnets, MIT, DOE/PC-70512-7.
4. Analysis Report, Develop and Test an Internally Cooled Cabled Superconductor (ICCS) for Large Scale MHD Magnets, MIT, January 1986, DOE-PC-70512-5.
5. Thome, R.J. and Tarrh, J.M., MHD and Fusion Magnets: Field and Force Design Concepts, John Wiley and Sons, Inc. 1982.

6.0 List of Symbols

A	amperes
kA	kiloampere (10^3 A)
MA	megampere (10^6 A)
T	tesla (10^6 gauss), magnetic field
m	meter(s)
cm	centimeters(s)
g	gram(s)
kg	kilogram(s) (10^3 g)
K	degrees Kelvin
TUS	tensile ultimate strength
TYS	tensile yield strength
psi	pounds per square inch
Pa	pascal (1 newton/square meter)
MPa	megapascals (10^6 Pa)
tonne	metric ton (10^3 kg)
in	inch
lb	pound
N	newton
s	second(s)
W	watts(s)
Ω	ohm
R	resistance, electrical
DC	direct current
L	inductance, electrical
V	volt
Cu	copper
J	joule

mJ	millijoule (10^{-3} J)
Nb_3Sn	niobium tin
NbTi	niobium titanium
MHD	magnetohydrodynamic
ICCS	internally cooled, cabled superconductor
σ	stress
p	pressure
atm	atmosphere(s)
I	current, electrical
I_c	critical current
H	enthalpy (thermodynamic)
H	henry, inductance, electrical

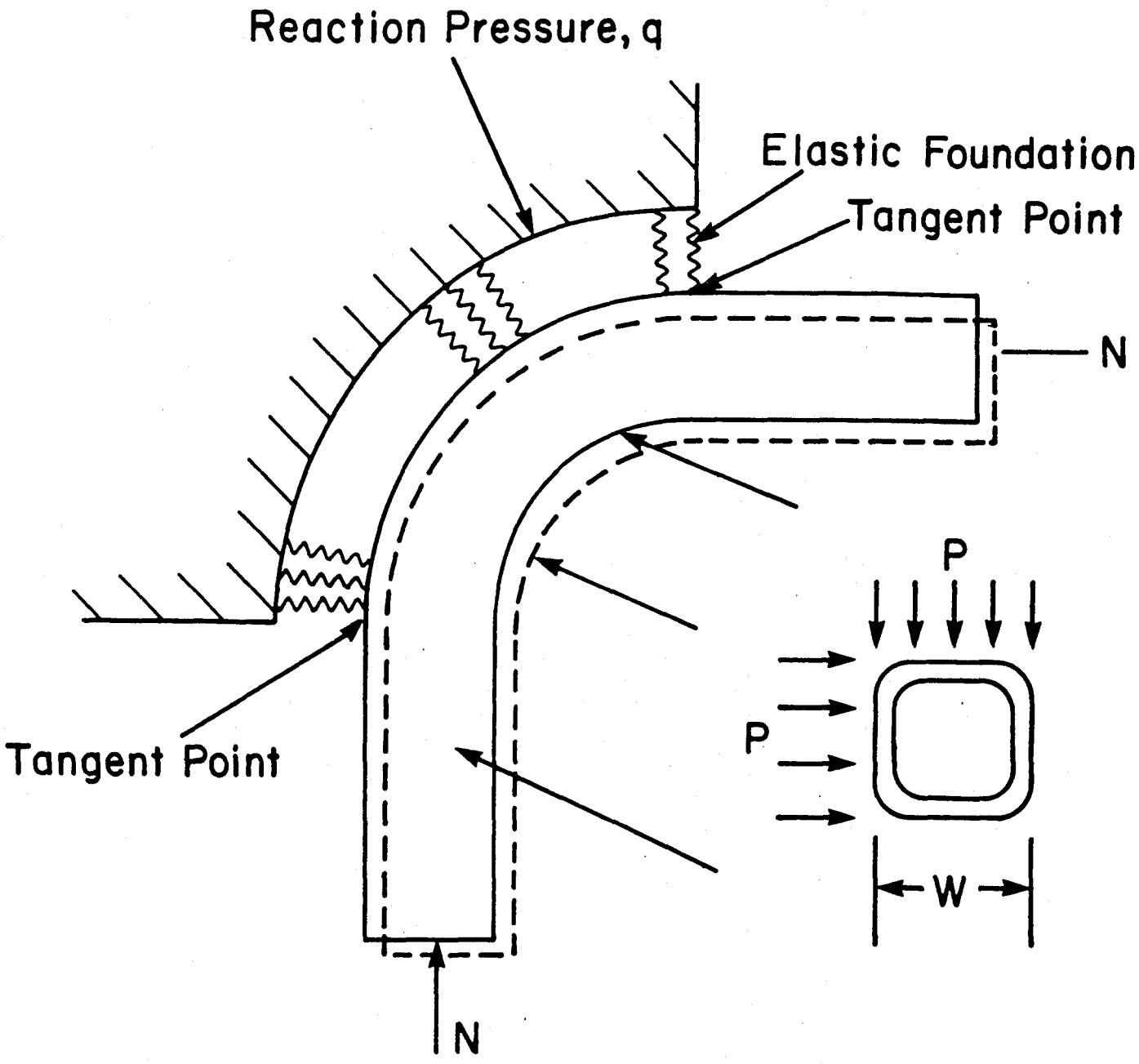

Fig. 1 – Representation of Corner Load Reacted by Elastic Foundation

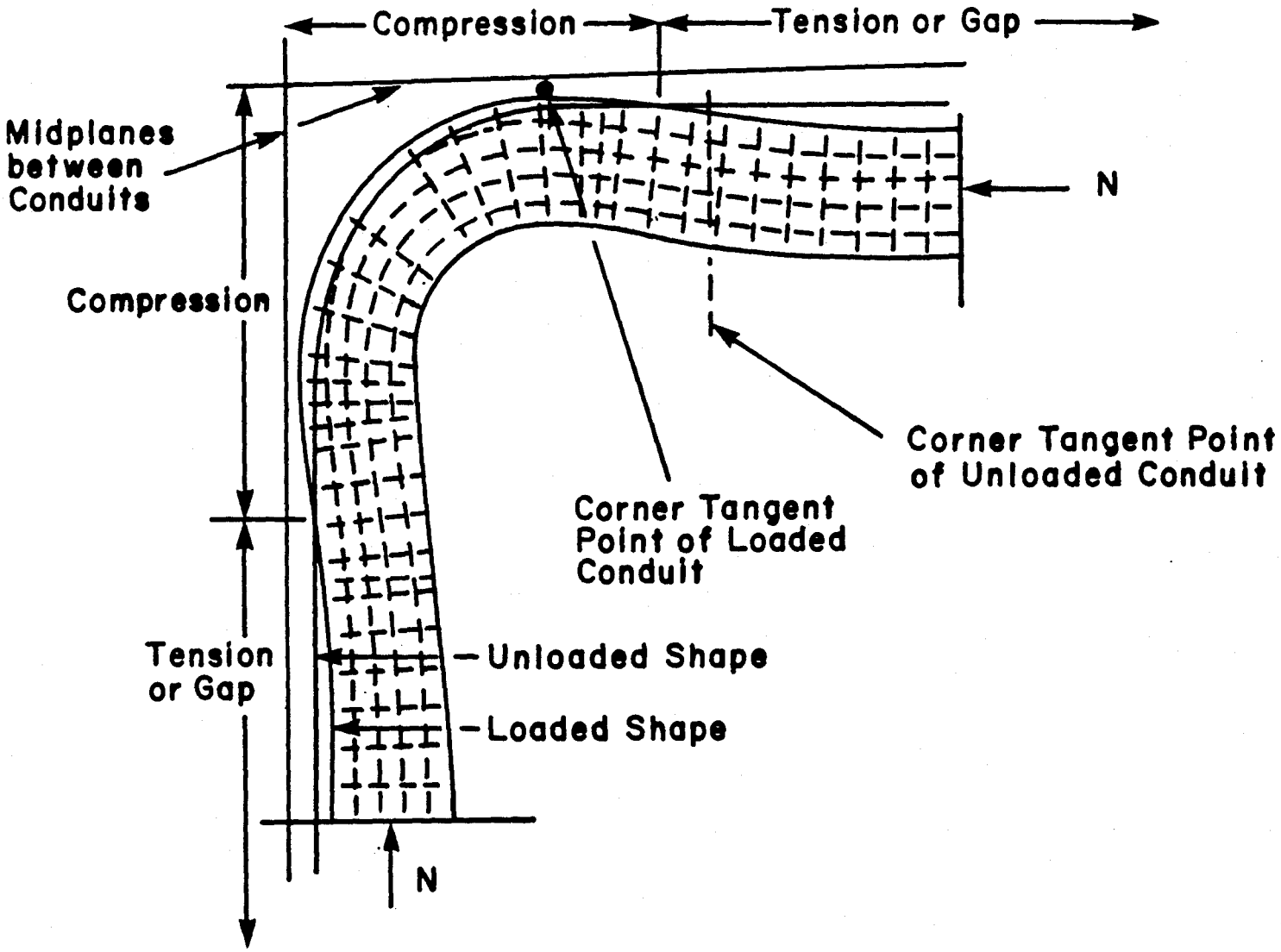

Fig. 2 – Corner Movement and Deformation

Fig. 3 – Geometrical Shape of 1/4of the Loose Conductor

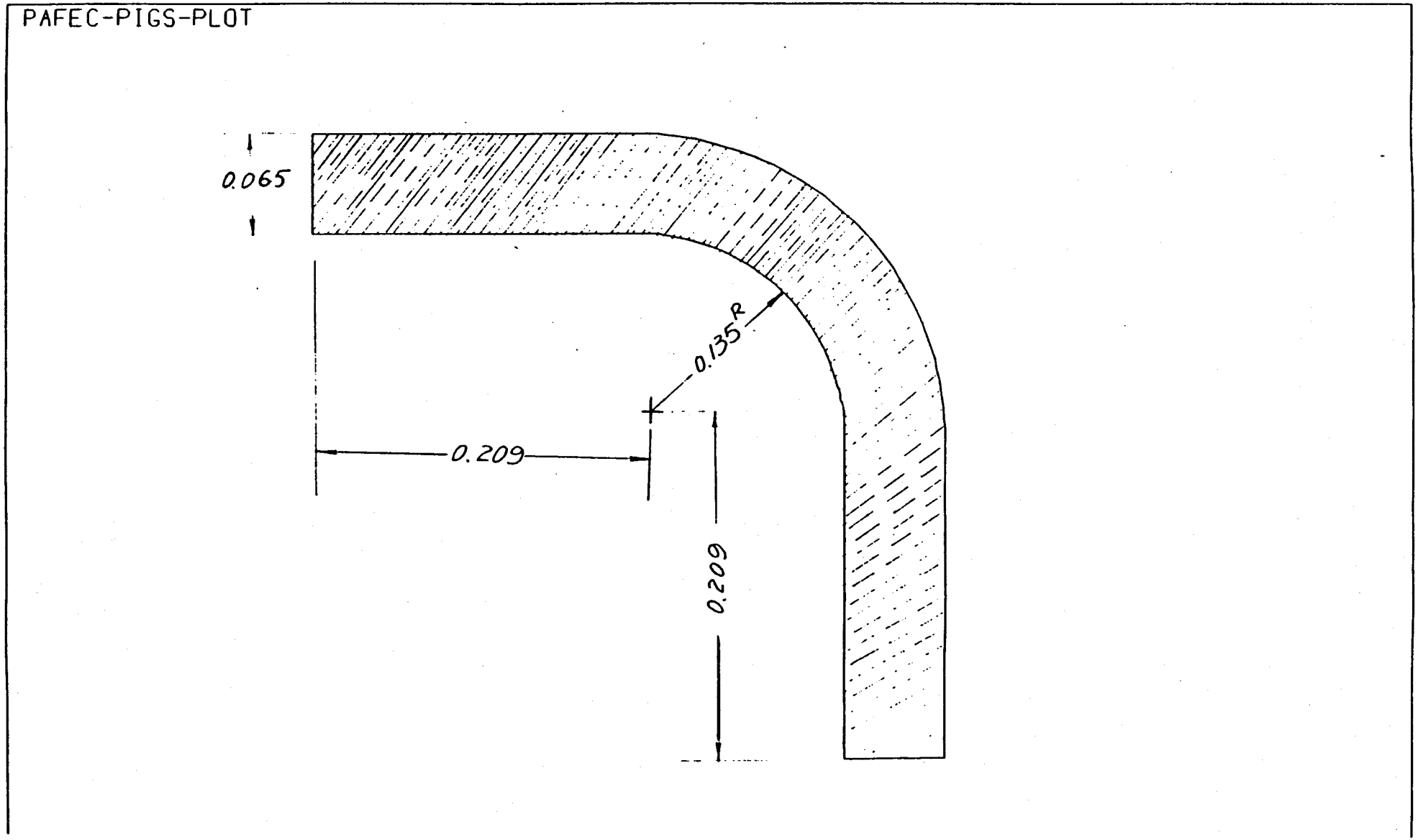

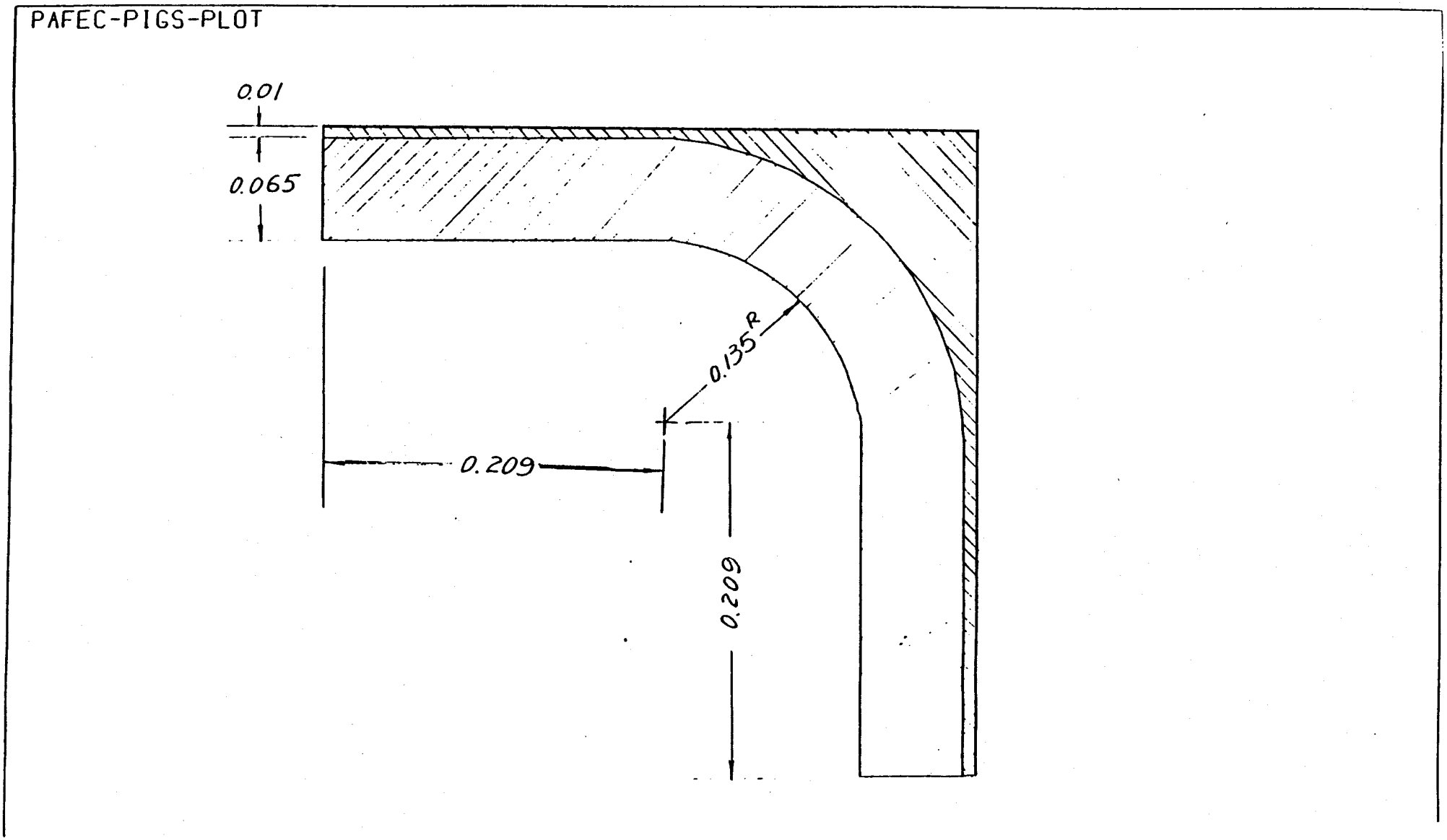

Fig. 4 – Epoxy Potting of the Conductor

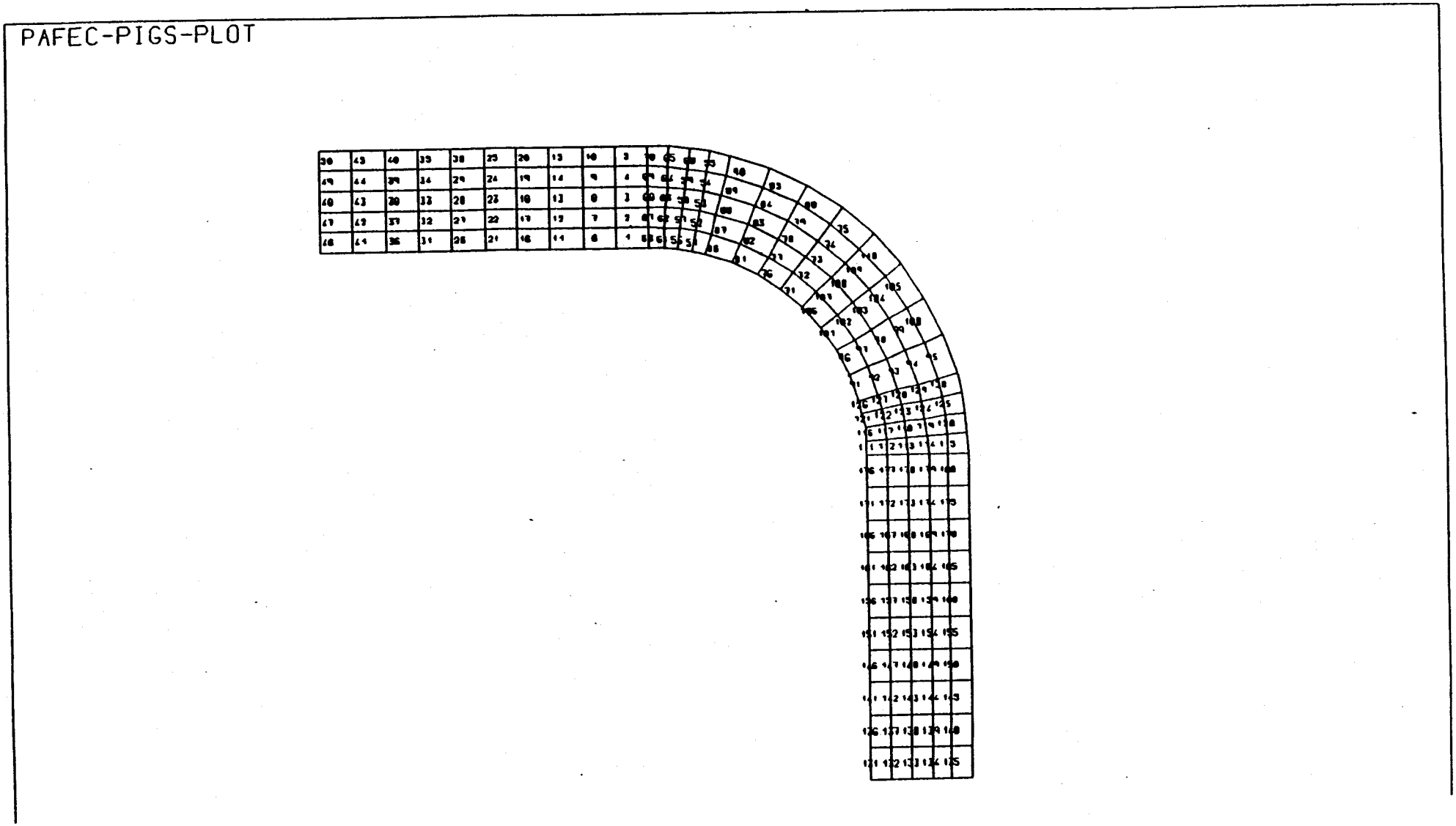

Fig. 5 – Element Numbers of the Loose Conductor

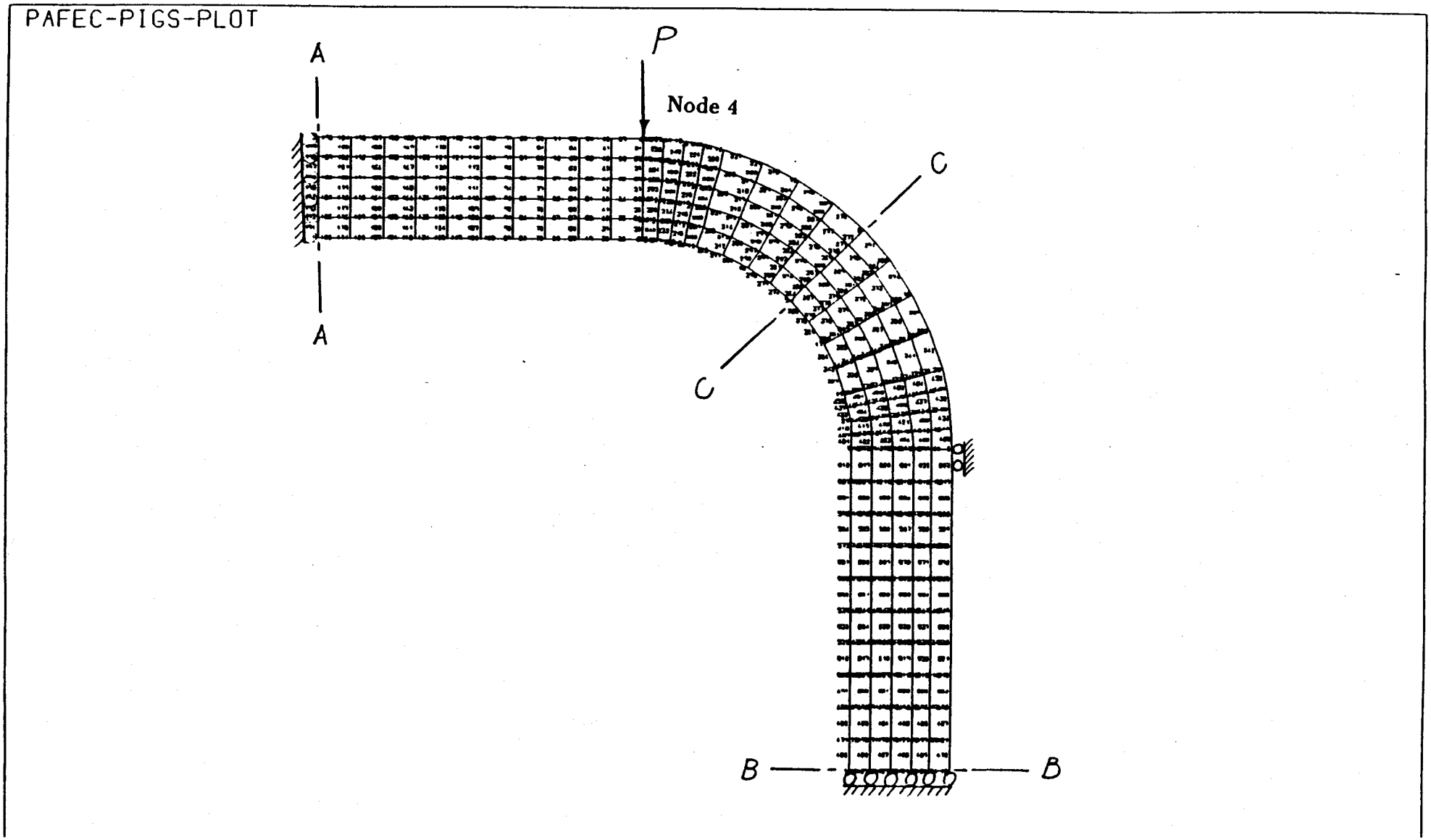

Fig. 6 – Nodal Numbers of the Loose Conductor

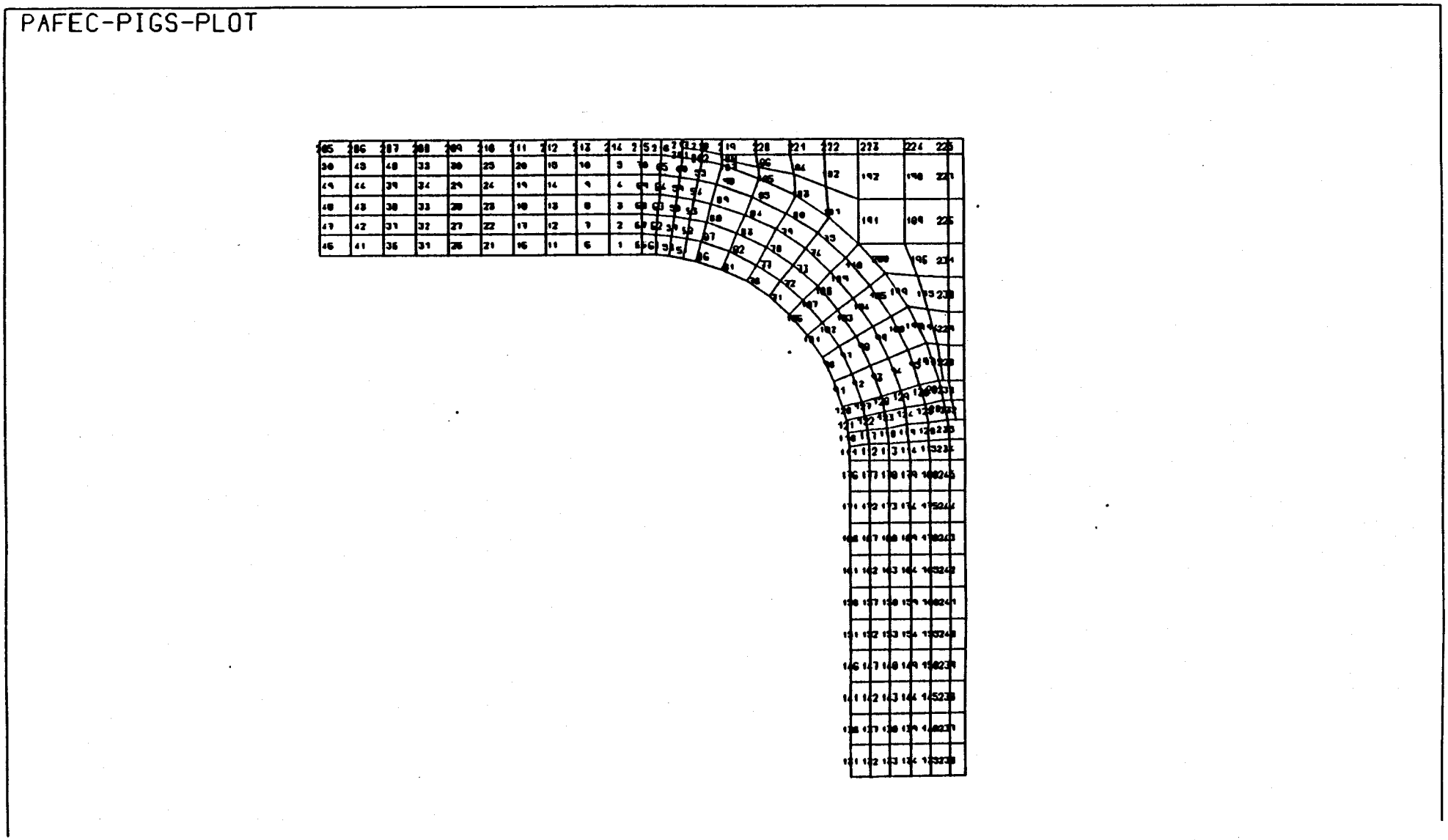

Fig. 7 –Element Numbers of the Potted Conductor

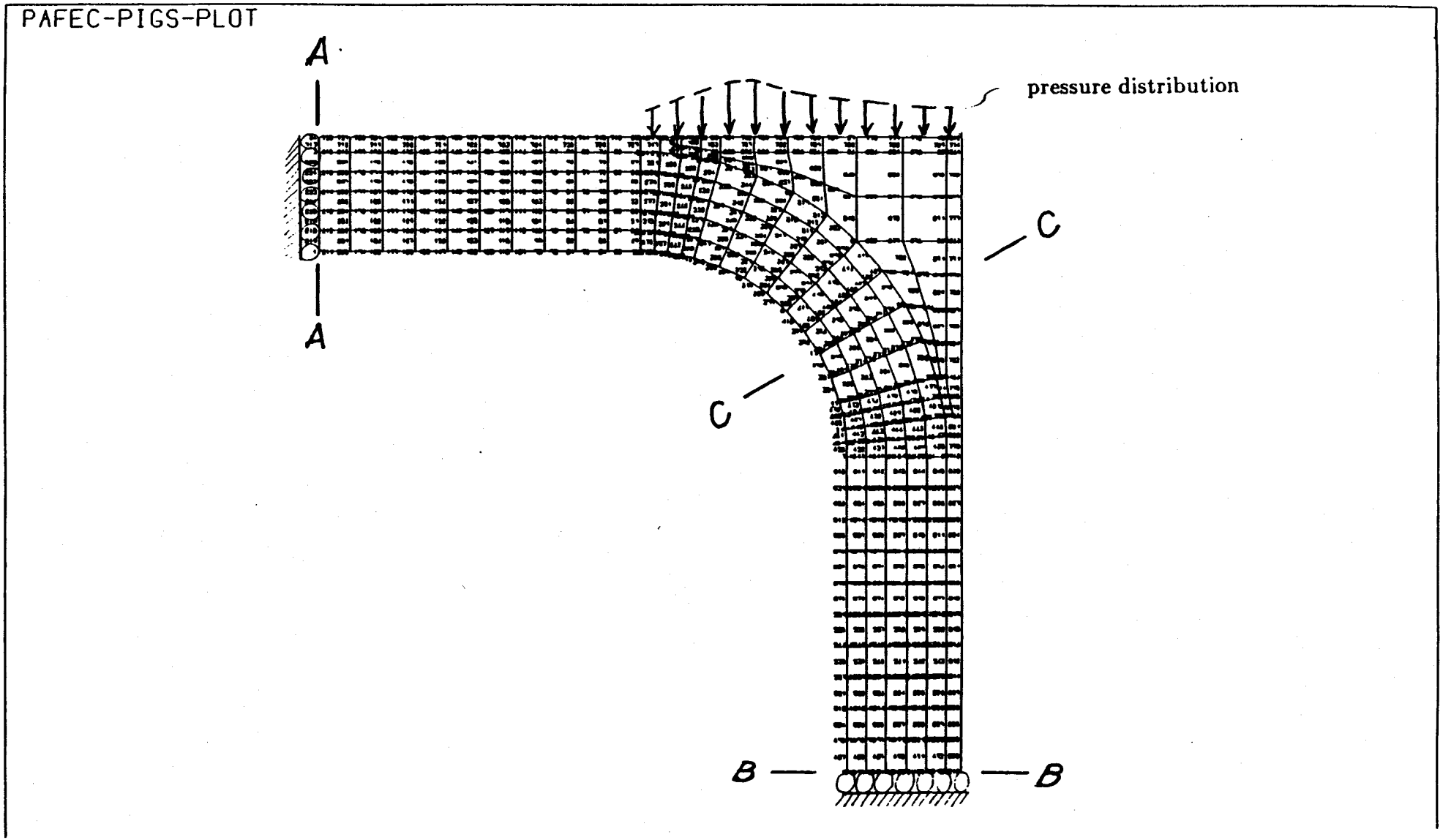

Fig. 8 – Nodal Numbers of the Potted Conductor

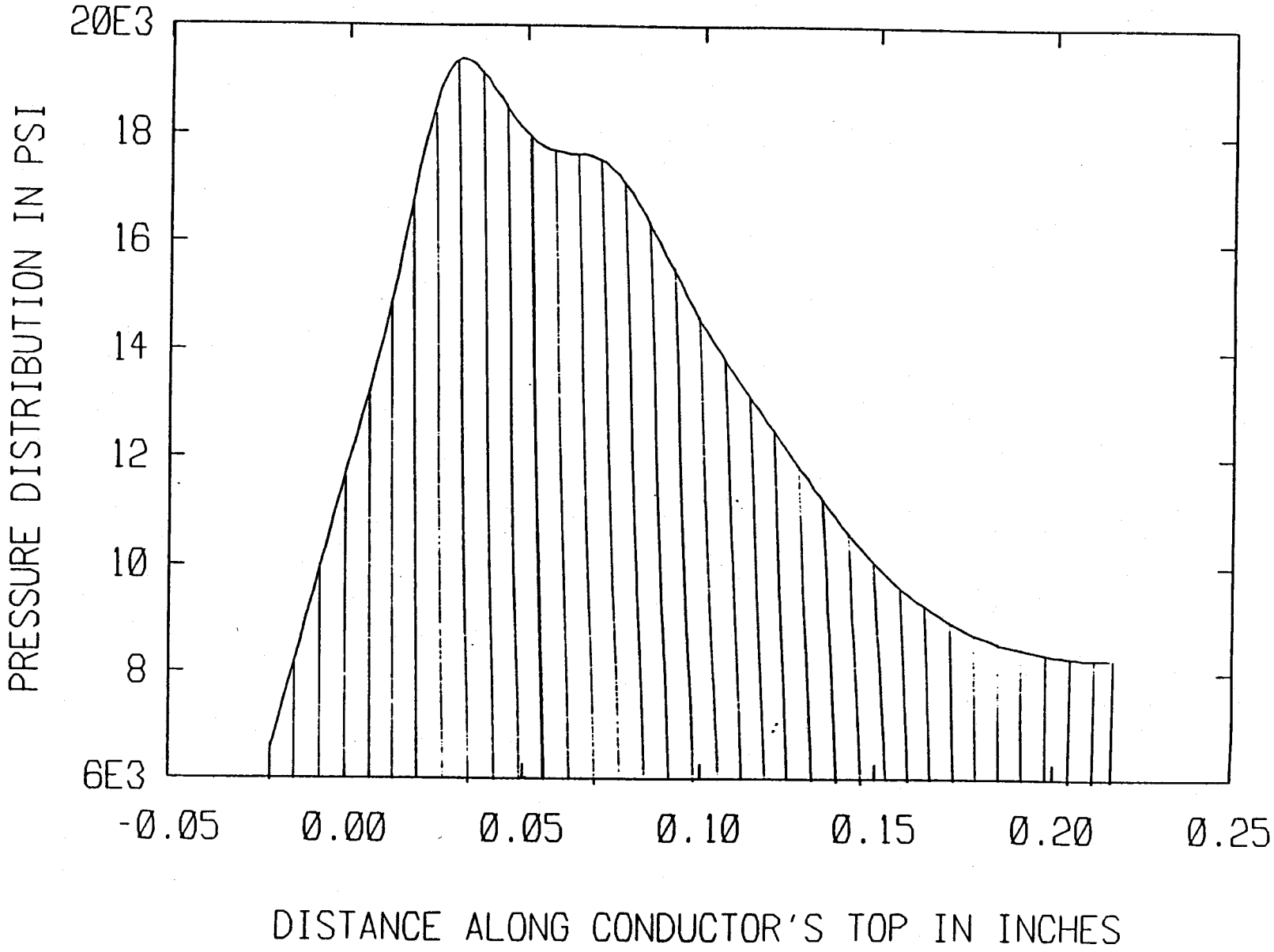

Fig. 9 – Load Distribution On Top Surface of the Potted Conductor

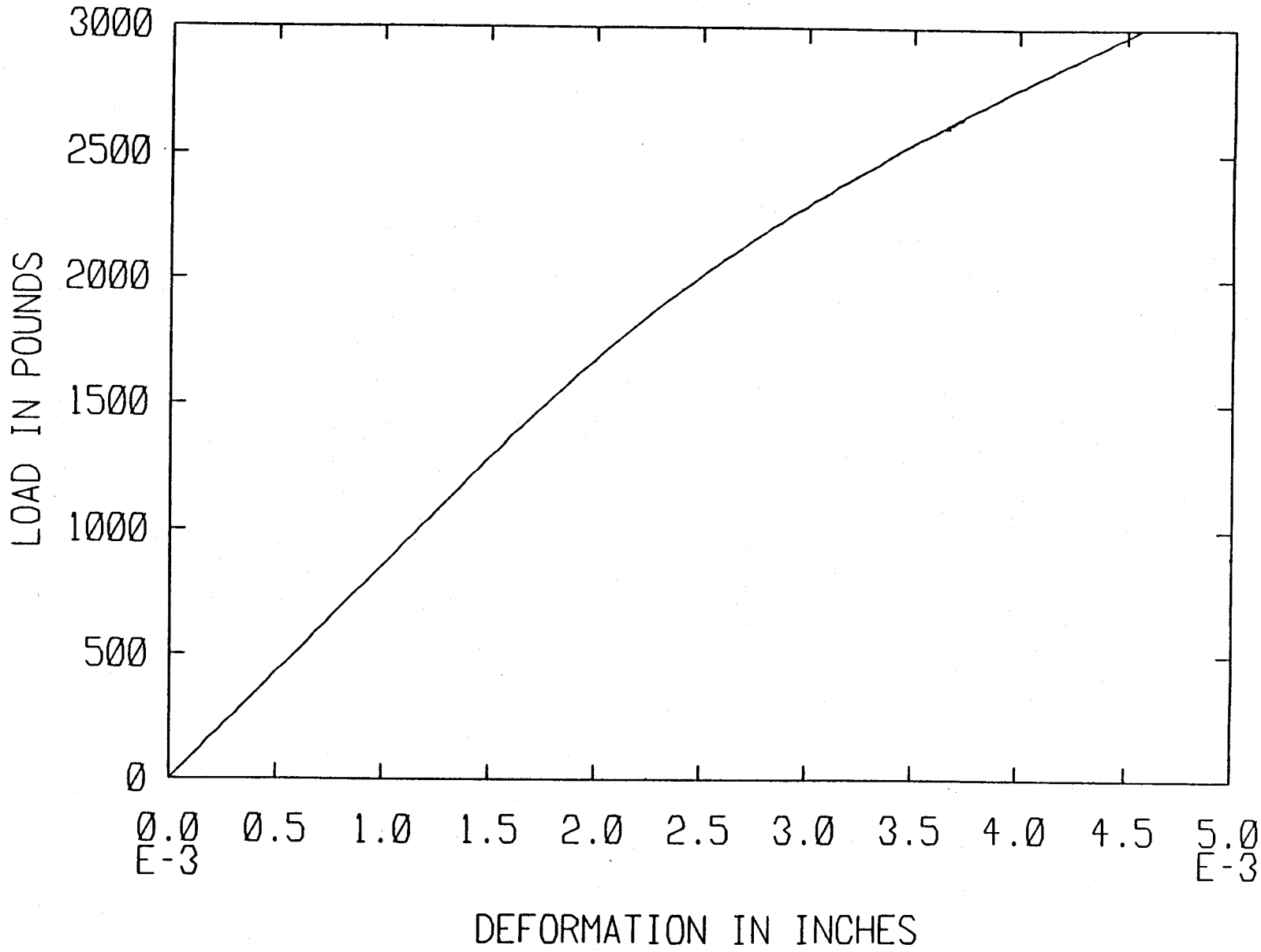

Fig. 10 – Force Deformation Curve of the Loose Conductor with Rigid Side Supports

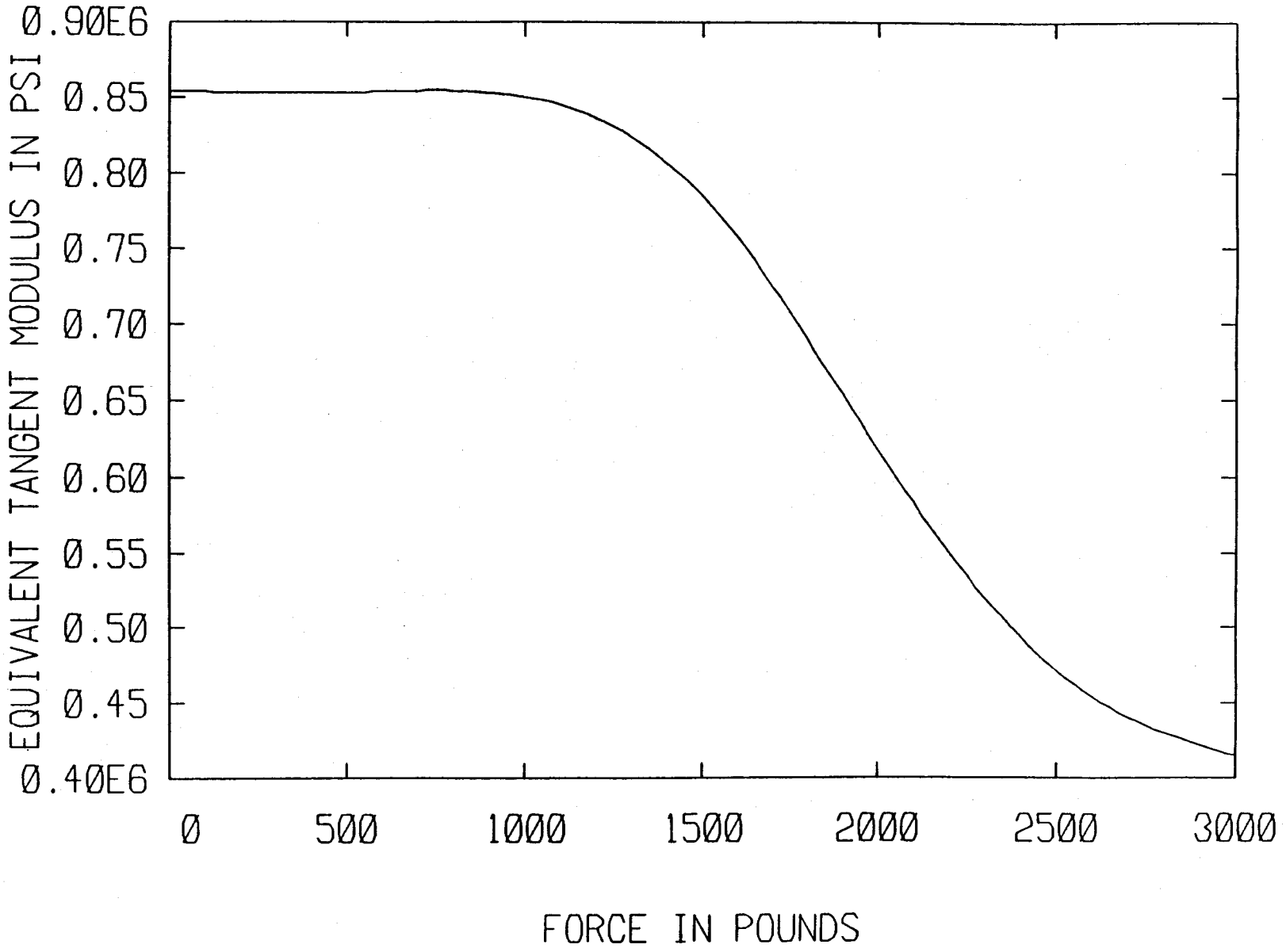

Fig. 11 – Equivalent Tangent Modulus-Force Curve of the Loose Conductor with Rigid Side Supports

Fig. 12 – Variation of Equivalent (von Mises) Stress Across the Critical Section of the Loose Conductor with Rigid Side Supports

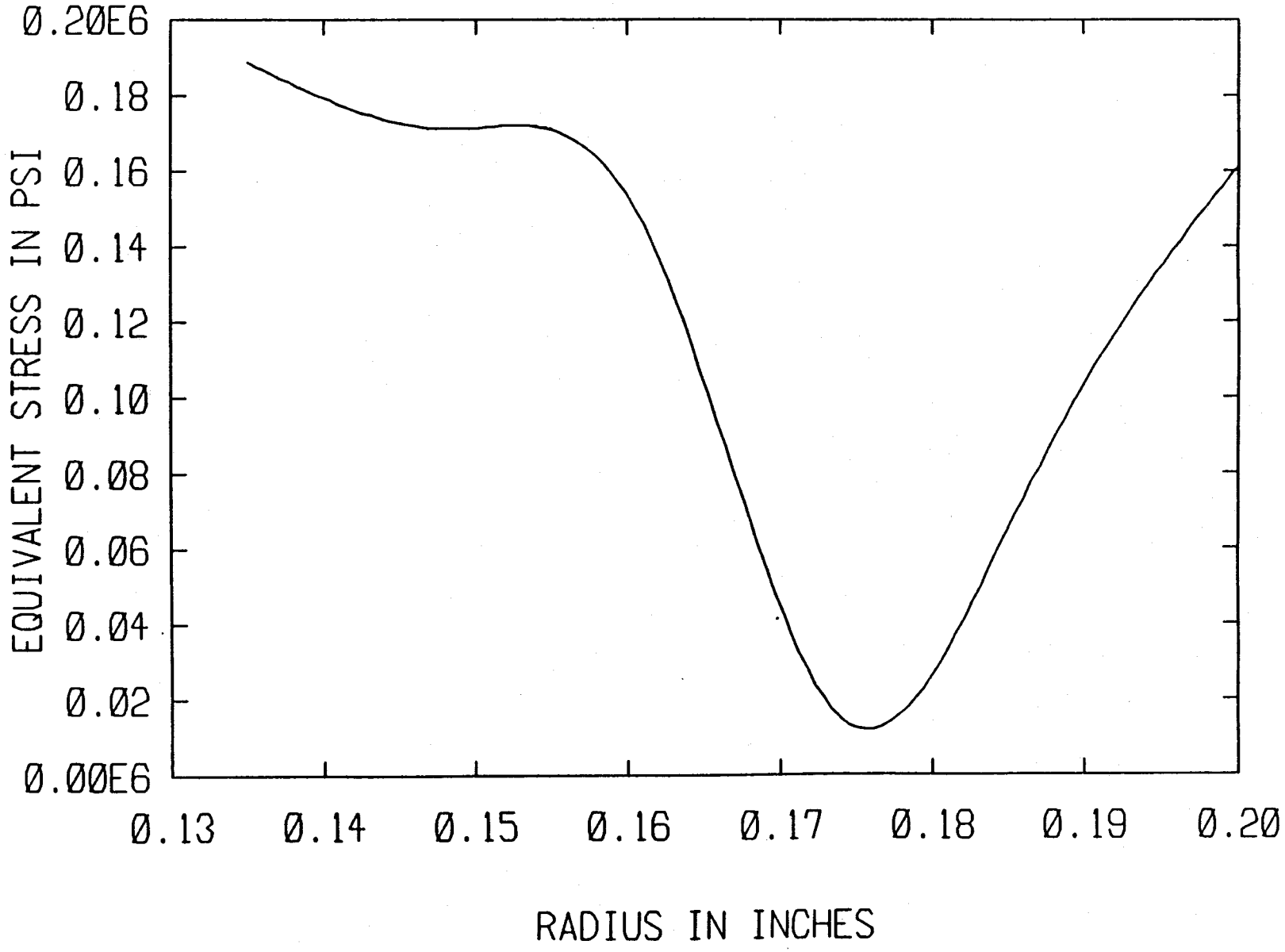

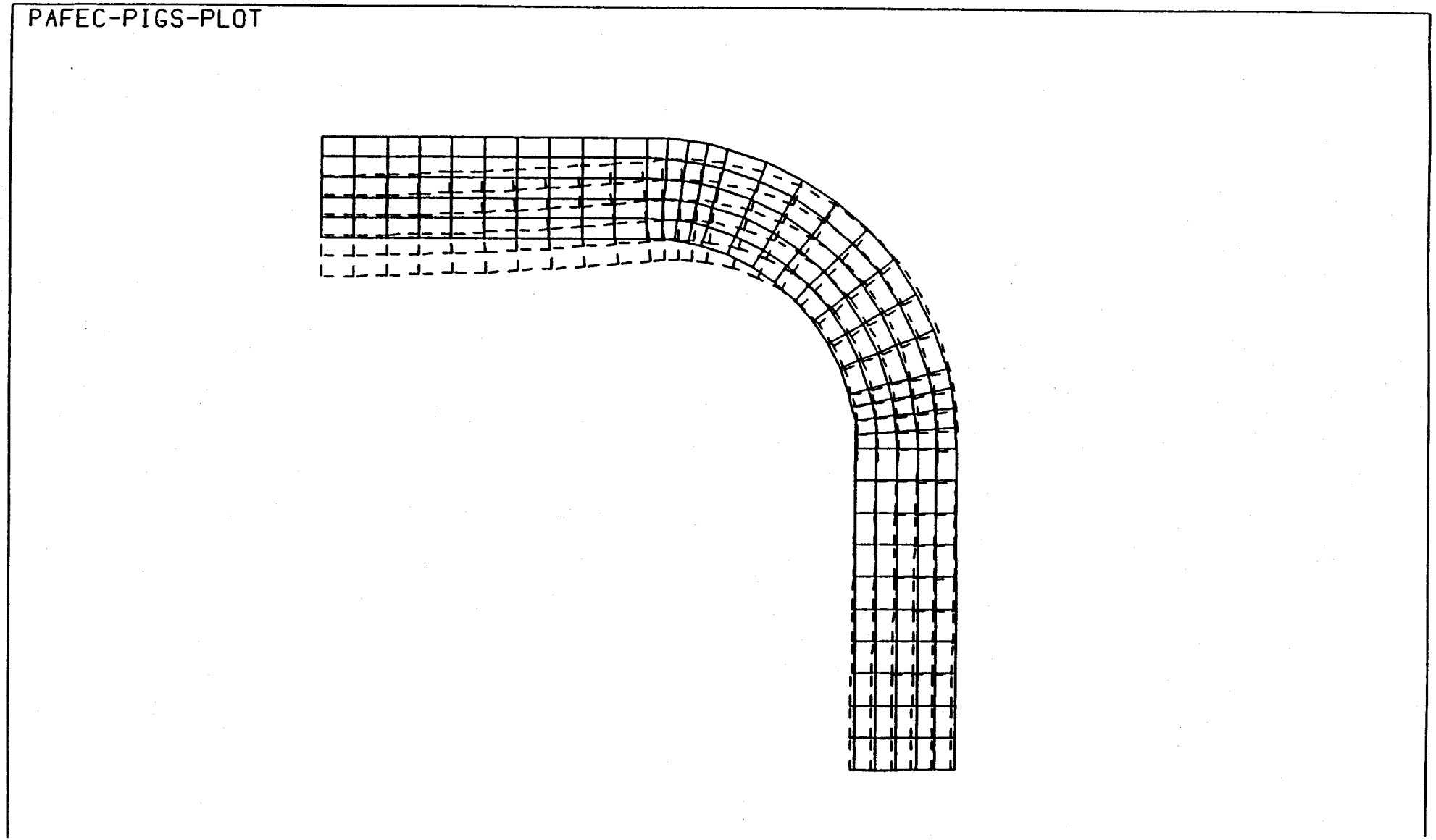

Fig. 13 – Deformation Shape of the Loose Conductor with Rigid Side Supports

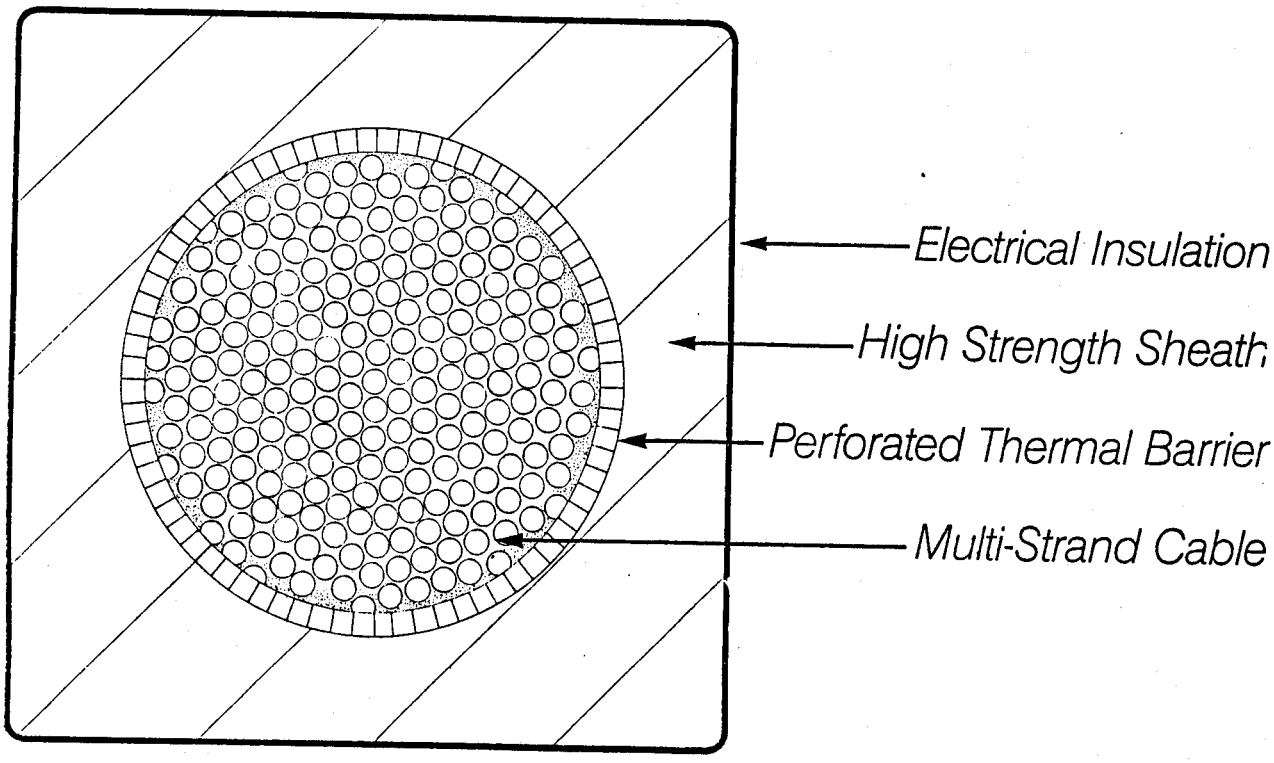

Fig. 14 – Proposed ICCS for DC Applications

ATTACHMENT A

PRELIMINARY DRAFT TEST PLAN

DRAFT

TEST PLAN

INTRODUCTION

The experimental program will be carried out with subscale conductors consisting of subelements of the proposed full-scale conductor. The basic element of a cable is a triplet which is simply a bundle of three wires twisted together. The first tests will be to determine the stability of these cable subelements using two different conductor designs. One will consist of three wires, each of which will be a multifilamentary composite. The other will consist of three wires in which only one of the three strands is a multifilamentary composite while the other two strands are pure copper. The overall copper-to-superconductor ratio in each of these triplets will be approximately the same. Preliminary tests have indicated that the latter configuration (the two copper strands and one composite strand triplet) will have the same performance as the triplet in which all three strands contain superconductor. If detailed tests confirm this indication, it will be possible to reduce the manufacturing cost of the proposed full-scale ICCS conductor substantially.

The first subscale cable to be tested will have 27 strands (9 triplets). This ICCS configuration in the finished condition will have overall dimensions of approximately 4 mm dia. The stability, quench propagation and internal pressure dynamics of this conductor will be tested in both short sample and small coil configurations in the background field of the high field test facility at MIT's National Magnet Laboratory. Results of these tests will be compared with predictions. We anticipate that the correlation between predictions and experimental results will be adequate to proceed with the procurement of long-term materials for the full-scale test conductor.

Full-Scale Test

The proposed baseline design assumes as 486-strand conductor encased in a stainless-steel sheath having overall dimensions of approximately 2.5 cm square. An approximately 15 m length of this conductor will be wound into a coil in a configuration closely duplicating the actual operating environment of a large-scale MHD magnet. This coil will be tested while monitoring its performance with respect to stability, quench propagation and pressure dynamics.

The final test performance analysis will include definition of the program, time, and cost to fully develop the manufacturing technology required for minimum risk construction of a large-scale MHD magnet.

Predictive Analysis

An attempt will be made to predict analytically the performance of the subsize conductors in the test configuration described in the next section. This analysis will address problems of transient stability having sudden energy inputs in the range of 100 microseconds to 100 milliseconds and steady-state stability having energy inputs over long periods of time (1 s to steady state). The maximum amount of energy that can be input into the conductor without causing a quench will be measured, and energy margins (mJ/cm^3) will be compared to predictions.

Similiarly, maximum hot-spot temperatures and pressures will be measured and compared.

The analysis will consider the differences in both electrical and thermal contact resistances between the two configurations; the slight differences in overall copper-to-superconductor ratios in the two trip-

let configurations, and also the inherently different filament sizes in individual strands (or strand in the case of the 2 and 1 cable) and therefore, different critical currents in the superconductor.

SCHEDULE

Tests will be performed in accordance with the schedule set forth in the Management Plan dated July 24, 1986.

SUBSCALE TESTS

Transient Stability

Good transient stability is one of the principal advantages of ICCS conductors. In the proposed geometry, at least 80% of the wire periphery is in contact with the coolant. Wire diameter is small and a large heat transfer area is thus achieved. Coolant is single phase, supercritical He. Under steady-state conditions a modest flow of supercritical helium through the high surface area ICCS conductor provides adequate stability. Under transient (0.1 to 100 ms) heating conditions ICCS cooling is dramatically enhanced by the so-called "Kapitza heat transfer,"[1] making transient stability uniquely independent of coolant flow.[3]

The purpose of this series of proposed experiments is to evaluate the limits of transient stability, in candidate, subsize, copper-stabilized NbTi ICCS test conductors. Figure 1 shows a 3.5 m length of a 27-strand, stainless-steel-sheathed ICCS conductor, wound into a noninductive test coil. Figure 1 also shows electrical terminations (top) and coolant couplings (left of terminations). The placement of the test coil is illustrated in Fig. 2. It can be seen here that the coil sits in the annulus between a set of two concentric pulse coils. Figure 2 illustrates electrical systems and instrumentation while Fig. 3 shows the helium system schematically. To provide the required transient heating, a capacitor is discharged into the pulse coil set. A double pulse used for Nb_3Sn is shown in Fig. 4. The double pulse was needed for the Nb_3Sn test conductor, because of its higher energy margin. Critical energy input for Nb_3Sn and NbTi cabled superconductors is compared in Fig. 5. Our

expectation is that the proposed NbTi ICCS conductors will have adequate transient stability for DC applications, such as MHD.

Protection

Transient stability assumes the sudden (0.1 to 100 ms) release of energy, able to drive the superconductor temporarily into its normal, resistivity state, but followed by recovery. Since heat transfer between wire and coolant is very high, the duration of the resistive heating period is extremely short. It is therefore postulated that transient recovery is so short that current transfer to the "all-copper" strands does not take place. The question is therefore: "What is the minimum amount of stabilizing copper which must be included in close proximity to the superconducting filaments?"

In the case of protection, on the other hand, it is assumed that the conductor has ceased to be superconducting. Current must transfer to the (now) less-resistive stabilizing copper, located in both the multifilamentary strand and in the pure copper strands. Since adequate voltage is available under these conditions, we hypothesize that the "all-copper" strands will participate fully in the protection process.

To protect ICCS from overheating, it must be provided with the following:

(i) An adequate amount and quality of stabilizing copper to minimize heating during shutdown. The quality of the copper is defined in terms of the effective Residual Resistivity Ratio (RRR). RRR = 100 is readily available.

(ii) A "quench detection" system designed to detect the existence of a normal zone anywhere within the coil winding.

(iii) A switch to cut off the DC power supply.

(iv) A shunt connected "Dump Resistor" to absorb the magnetic stored energy and provide an adequately short current-decay time constant, to limit the ICCS conductor "Hot-Spot" temperature to a safe value.

A "Protection" test of the subsize ICCS test conductor can be readily carried out by voltage measurement across the full (3.5 m) length of the conductor as it is driven into a quench.

Specific Test Conductor and Test Characteristics

Two 3.5-m-long, 27-strand ICCS test conductors will be fabricated. Type A will consist of 27 identical strands of a 0.510 mm diameter wire with a 7:1 Cu:NbTi ratio. Type B will consist of 9 strands of a 0.510 mm diameter wire with a 1.35:1 Cu:NbTi ratio and 18 strands of a 0.510 mm diameter pure copper wire, arranged in nine (9) wire triplets, each consisting of one NbTi/Cu strand and two pure Cu strands. The overall Cu:NbTi ratio for this cable is thus 5.2:1. Each cable will now be double wrapped with 0.025 mm thick stainless steel foil and will be reduced to a 3.4 mm diameter bundle. Each cable will then be pulled through a 3.5 mm ID stainless steel tube with an 0.38 mm thick wall. The encapsulated conductor will then be drawn down to a tube of 4.05 mm OD, thus ensuring a 34% He fraction in the cable.

The round, 4.05 mm diameter conductor will then be wound into a single layer, 83 mm ID noninductive (bifilar) coil, designed to fit in the annular space between two existing, coaxial pulse coils and will be secured within the pulse coil assembly by means of paraffin wax potting.

The two test-coil assemblies will be mounted on support probes for insertion into an existing LHe-cooled, LN_2-shielded dewar. Special pre-

cautions must be taken to provide structural support of the coil assembly, due to large eccentric forces generated. Both ends of each conductor will be terminated for low-loss connection to 2,000 A current leads as well as helium plumbing connectors.

Operating characteristics of the two test conductors are as follows:

CONDUCTOR	A	B	
Critical Current (I_{crit}) @ 5 T	810	1,125	A
Critical Current (I_{crit}) @ 8 T	459	720	A
Multifilamentary strand Cu:NbTi ratio	7:1	1.35:1	
Overall Cu:NbTi ratio	7:1	5.2:1	
EXPECTED ENERGY MARGIN			
Limit at I_{op}/I_{crit} =	0.8	0.8	
Namely I_{op} =	367.	576	A
at B = 8 T	50	35	mJ/cm^3

Test operations will be carried out as follows:

The test coil is first mounted on its probe an then inserted into the appropriate (150 mm OD) dewar. The dewar is then inserted into the background field coil at the Francis Bitter National Magnet Laboratory. This is an 8 T peak on-axis solenoid of Bitter plate construction. After appropriate cooldown and dewar backfill with liquid helium, the background field is raised to the desired field level. Field levels of interest will range between 4 and 8 teslas. Helium pressure in the ICCS conductor itself will be maintained at 2.5 to 3 atm. - that is, in a supercritical,

single phase state. Cooldown without mass flow between test runs is assured since the ICCS conductor is immersed in a liquid helium bath.

Our objective is to determine the energy margin (Q) of an ICCS conductor operating at a given field (B) as well as at a given current level (I_{op}). After having established the appropriate field, B, the procedure then calls for the establishment of the operating current, I_{op}. The transient energy pulse is delivered to the ICCS conductor inductively by means of the pulse coil set (see Figs. 2, 3 and 6). In order to energize the pulse coil, a capacitor must be charged to some predetermined level (such as 100 V). The test run takes place with the discharge of the capacitor into the pulse coil. This will be done using a half-cycle (single) pulse, lasting 100 ms. The amount of energy which is inductively coupled into the test coil is known from extensive calibration tests. Voltage taps across the test conductor will indicate whether or not the conductor recovers or goes normal (quenches). Several discharge runs must be performed to narrow the range between recovery and nonrecovery.

It is expected that transient stability of the Type A ICCS test conductor will be higher than that of Type B, because all strands have copper in intimate contact with the superconductor. Since MHD conductors usually operate under steady state, DC conditions, the Type B conductor, however, should have adequate transient stability. It also has the minimum Cu:Sc ratio identified by the previous design and performance requirements analysis. It thus represents a minimum cost configuration. Separate "ramp" tests, in which the current will be ramped up from zero to maximum current at different, ever increasing rates, will also be performed. The objective of this test will be to determine whether or not there is any significant "Lorentz Compaction Heating" during magnet energization.

REFERENCES

1. S.R. Shanfield et al., "Transient Cooling in Internally Cooled Cabled Superconductors (ICCS)," IEEE Trans. Mag, MAG-17(5): 2019, 1981.

2. M.O. Hoenig, A.G. Montgomery and S.J. Waldman, "Cryostability in Force-Cooled Superconducting Cables," IEEE Trans. Mag, MAG-15(1): 792, 1979.

3. M.O Hoenig, "Internally Cooled Cabled Superconductors Part II," Cryogenics, August 1980.

4. M.O. Hoenig, "Internally Cooled Cabled Superconductors, Part I," Cryogenics, July 1980.

5. S. Dresner, "Protection Considerations for Force-Cooled Superconductors, Proc. 11th Symposium on Fusion Engineering, IEEE Cat. No CH2251-7, p. 1218, 1985.

6. J.R. Miller, L. Dresner, J.W. Lue, S.S. Chen and H.T. Yeh, "Pressure rise during the quench of a superconducting magnet using internally cooled conductors," Proc. 8th Int. Cryogenic Eng. Conf., IPC Science and Technology Press. Guilford, Surrey, UK, pp 321-329.

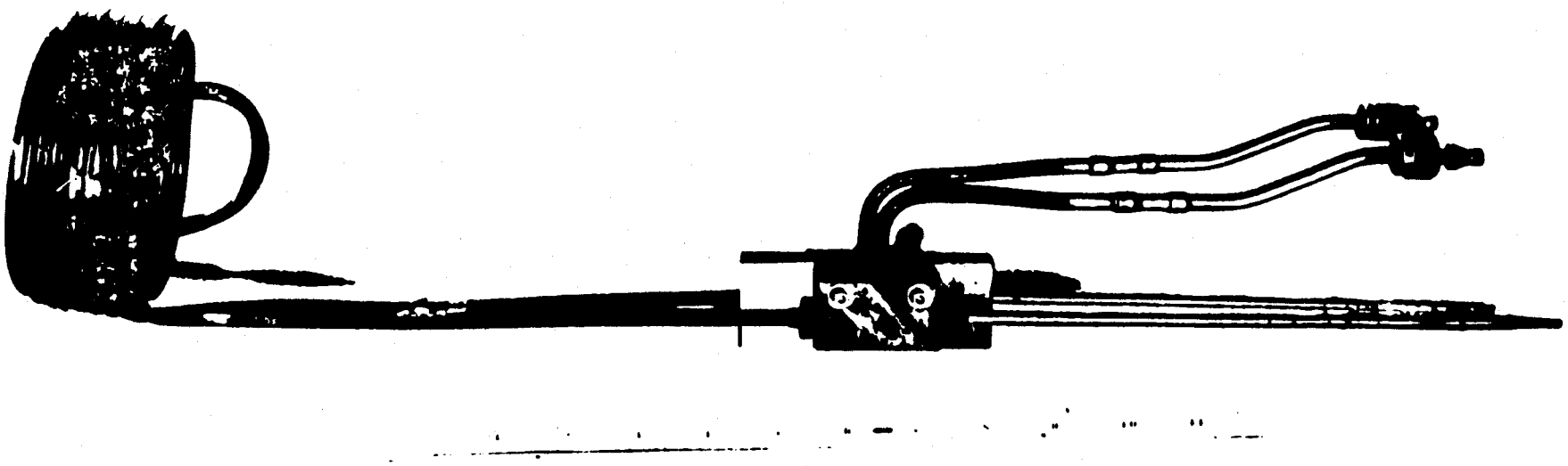

Figure 1. Stability test coil of subsize conductor showing bifilar winding and current terminations and helium connections.

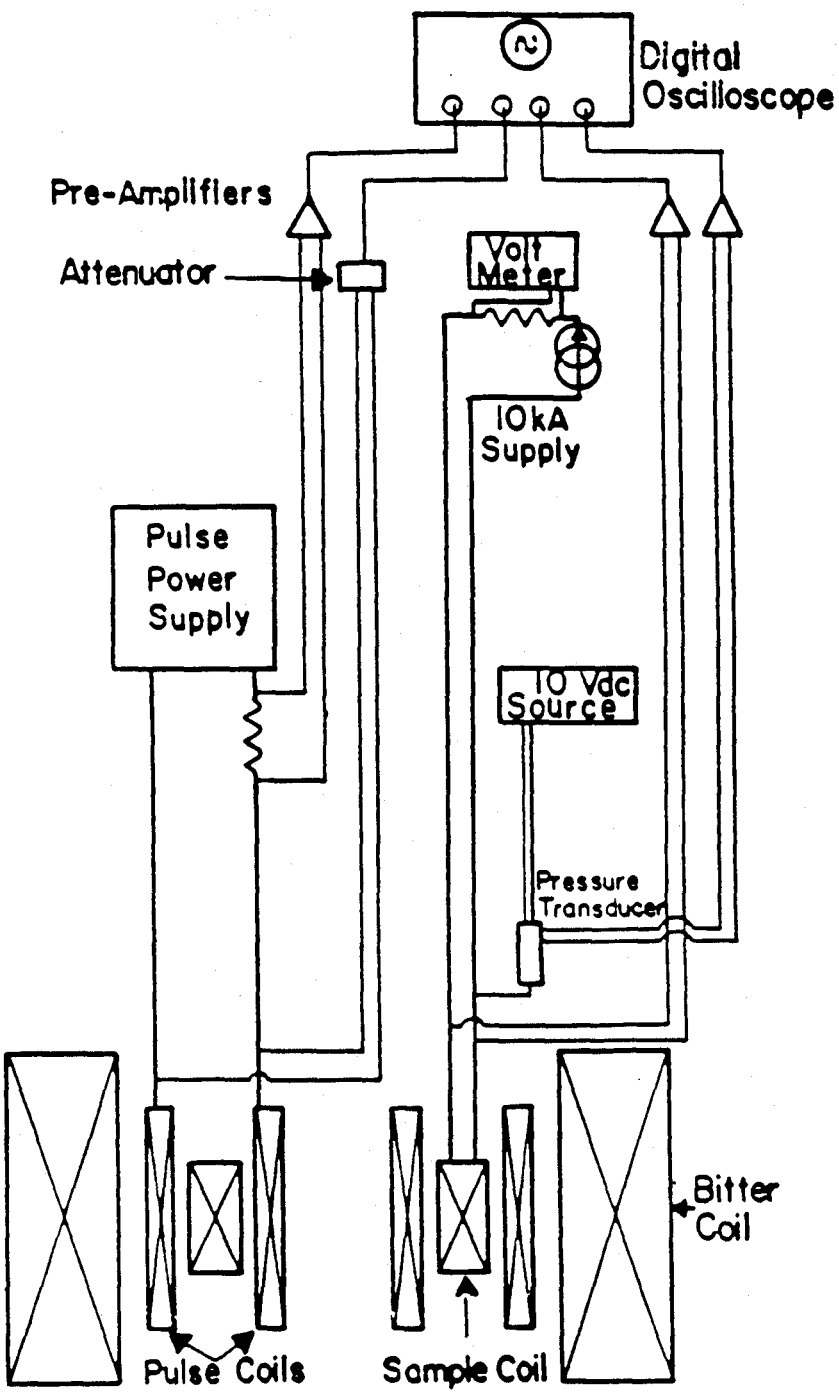

Figure 2. Schematic of the instrumentation and experimental set-up.

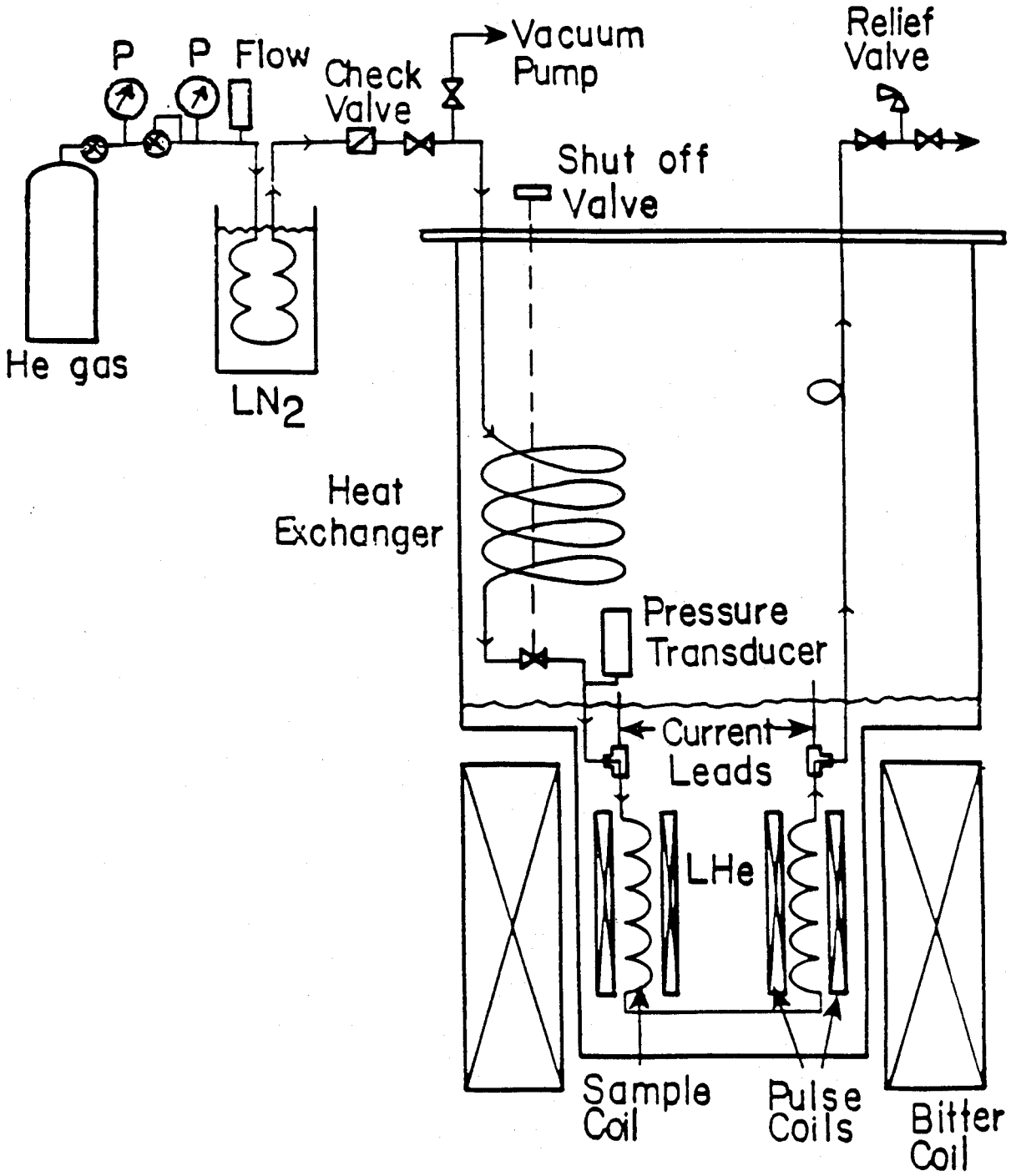

Figure 3. Schematic of the helium flow circuit.

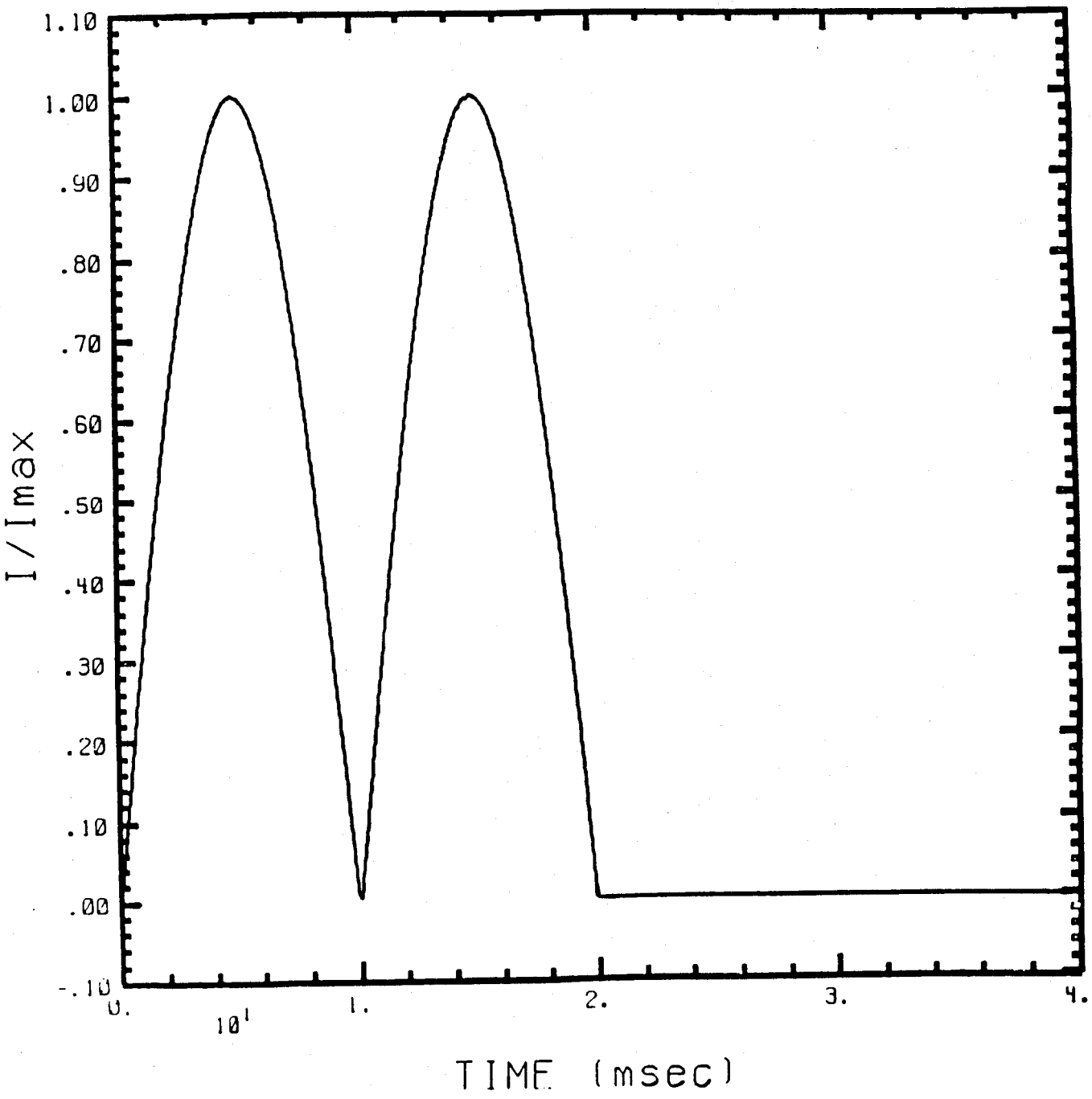

Figure 4. Inductive pulse. The double pulse was used for Nb_3Sn ICCS. A single pulse (Δt = 100 ms) would be used for NbTi.

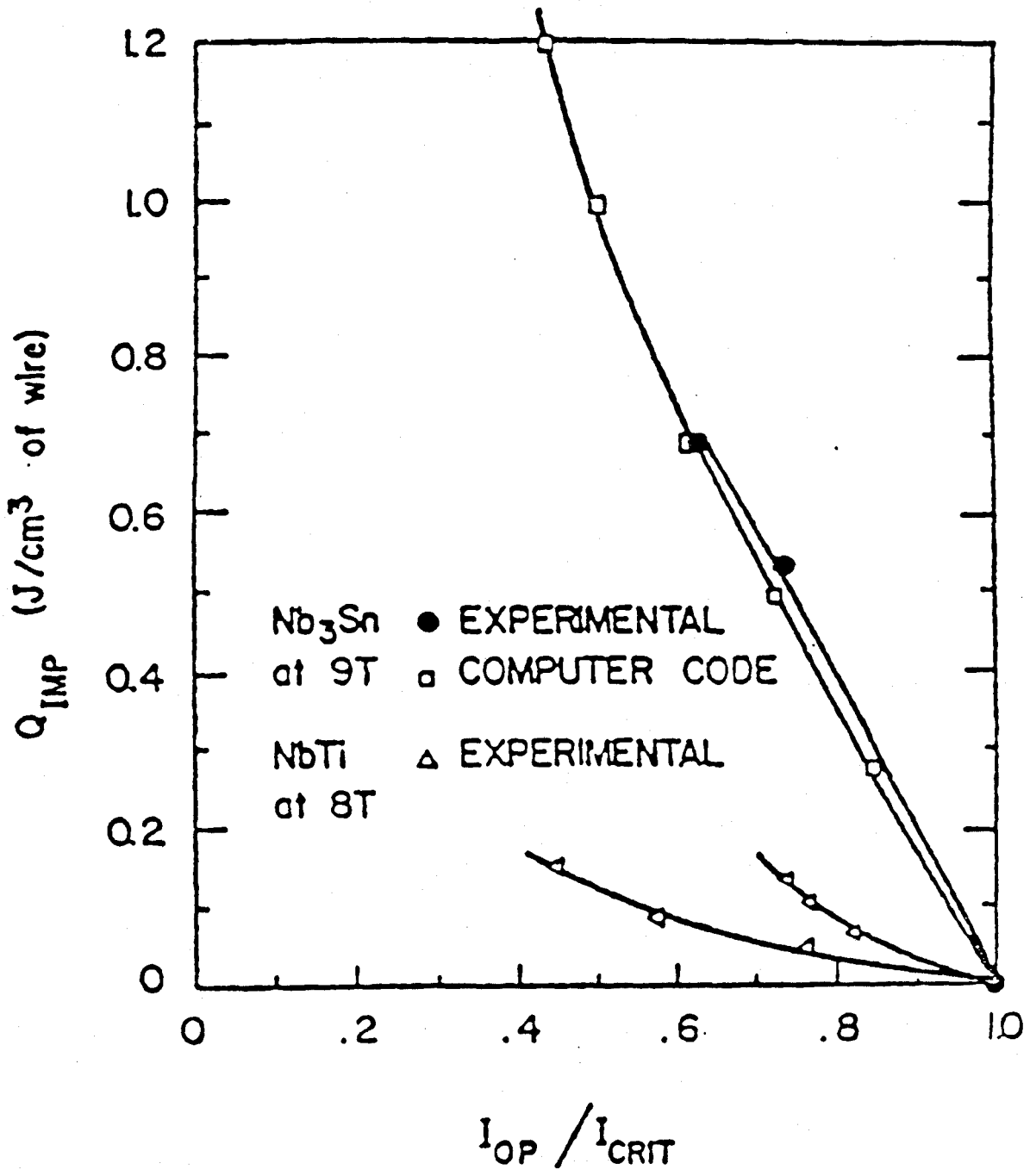

Figure 5. Critical energy input for NbTi and Nb_3Sn cabled superconductors.

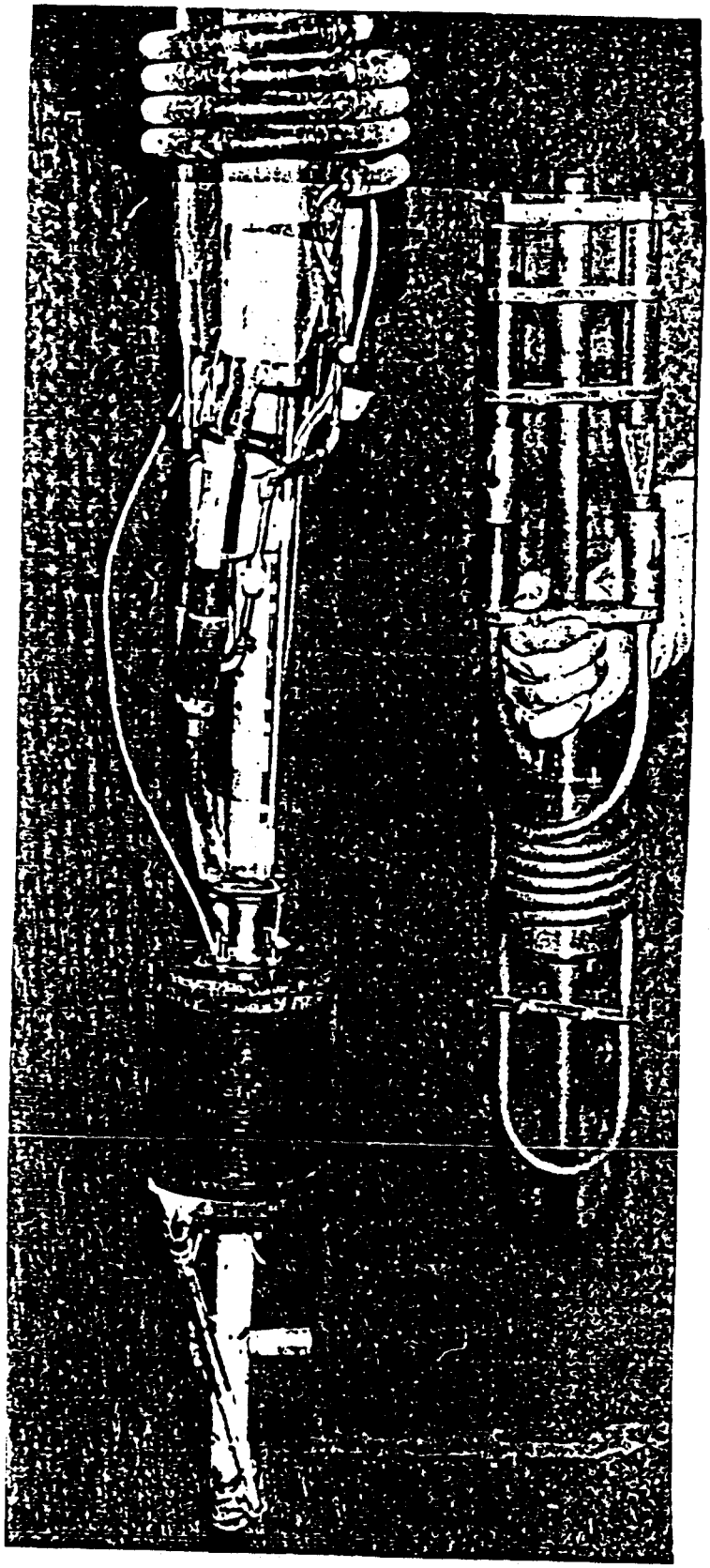

Figure 6. Six-inch-scale test coils: (i) NbTi test coil in pulse coil set – left, and (ii) test coil without pulse coil – right.